J Mater Sci (2010) 45:4029–4035
DOI 10.1007/s10853-010-4481-9

The effect of heat treatments on the creep–rupture properties of a wrought Ni–Cr heat-resistant alloy at 973 K

Manabu Tanaka · Ryuichi Kato

Received: 26 January 2010 / Accepted: 5 April 2010 / Published online: 20 April 2010

Abstract The effect of heat treatments on the creep–rupture properties was investigated on a wrought Ni–Cr heat-resistant alloy at 973 K. Short-time aging (aging for 3.6 ks (1 h) at 973 K) was made on the solution-treated specimens with different grain sizes. The fine-grained specimen (the grain diameter, $d = 45.2$ μm) produced by short-time solution treatment exhibited almost the same rupture life and superior creep ductility as those of the medium-grained specimen ($d = 108$ μm) produced by normal solution treatment. The fine-grained specimen and medium-grained specimen showed the longer rupture life compared with the specimen with recommended aging. The principal strengthening of specimens was attributed to the precipitation hardening by γ' phase particles. The fine-grained specimen had the highest hardness, and the increase of the hardness was observed in both the fine-grained and the medium-grained specimens during creep at 973 K. However, coarse-grained specimen ($d = 286$ μm) with high-temperature long-time solution treatment exhibited significantly short rupture life owing to insufficient precipitation hardening after the short-time aging and during creep. Ductile intergranular fracture with dimples occurred in the fine-grained specimen, while brittle intergranular fracture was observed in the medium-grained specimen and in the specimen with recommended aging. Both transgranular fracture and brittle intergranular fracture were observed in the coarse-grained specimen. A simple heat treatment composed of short-time solution treatment and short-time aging is applicable to high-temperature components of wrought Ni–Cr alloys.

M. Tanaka (✉) · R. Kato
Department of Mechanical Engineering, Faculty of Engineering and Resource Science, Akita University, 1-1 Tegatagakuen-cho, Akita 010-8502, Japan
e-mail: tanaka@mech.akita-u.ac.jp

Introduction

A wrought Ni–Cr (Inconel X-750 type) heat-resistant alloy has been used for rotor blades and wheels, bolts, and other structural components in gas turbines or high-temperature components in rocket-engine thrust chambers. This alloy is also used from sub-zero to about 923 K for springs and fasteners. Depending on the application and the properties desired, various heat treatments are employed. The higher solution temperature seems to give optimum creep–rupture properties, while the lower solution temperature is favorable for improved fatigue resistance (by finer grain size) or improved resistance to notch sensitivity [1]. Solution treatments plus double aging are generally employed for improved creep properties in wrought Ni–Cr heat-resistant alloys [2–6]. For a long-term service at temperatures above about 873 K, optimum properties of a wrought Ni–Cr alloy are believed to be achieved by solution treatment (about 1,423 K), plus stabilization treatment (about 1,123 K), plus precipitation treatment (about 973 K) [3]. It is well known that γ' phase with $L1_2$ crystal structure (typically $(Ni, Co)_3(Al, Ti)$) is the principal strengthening phase in Inconel X-750 alloy [7, 8]. Large precipitates of $M_{23}C_6$ carbide or γ' phase generally decorate the grain boundaries [7, 8].

The effect of grain size on creep properties has been investigated on many heat-resistant alloys [1, 4, 9–13]. The fracture mechanisms may also depend on the grain size and may affect the rupture properties of these alloys [10], although intergranular fracture is generally observed in high-temperature fracture of the heat-resistant alloys. In this study, the effect of heat treatments on the creep–rupture

properties was investigated using a wrought nickel-base (Inconel X-750 type) heat-resistant alloy at 973 K. The fracture mechanism was examined using an optical microscope and a scanning electron microscope (SEM) on the ruptured specimens with different grain sizes. The microstructure and precipitated phases were also examined using a transmission electron microscope equipped with EDS (TEM-EDS), or a scanning electron microscope equipped with EDS (SEM-EDS). The relationship between rupture properties and the microstructure was discussed.

Experimental procedure

A wrought Ni–Cr heat-resistant alloy was used in this study. The main alloy chemical composition is 0.06 mass% C–15.03 mass% Cr–2.43 mass% Ti–1.26 mass% Al–1.01 mass% Nb (+Ta)–7.48 mass% Fe–71.80 mass% Ni (+Co). The alloy was supplied in the form of hot-forged alloy bars of 20 mm in diameter. Heat treatments were performed on specimens of ~90 mm in length. Table 1 reports the heat treatment, the grain diameter, and the hardness of the heat-treated specimens of the Ni–Cr alloy. Specimens were water quenched after solutioning to prevent precipitation during cooling. Specimens with different grain sizes were obtained by solution heating for different durations at 1,423 K or 1,473 K, while solution heating for 7.2 ks (2 h) at 1,423 K is normally employed for this wrought Ni–Cr alloy. Solution treatments plus double aging are recommended for improved creep properties in wrought Ni–Cr heat-resistant alloys [2–6]. The heat treatment of the specimen with recommended aging for improved creep properties is also listed in Table 1. The solution-treated specimens and the specimen with recommended aging were then machined into creep specimens of 5 mm in diameter and 30 mm in gauge length. Creep–rupture experiments were conducted using single lever-type creep–rupture equipment with an electric furnace under the initial stress of 294, 343, or 392 MPa at 973 K in air. It took about 9.0 ks (2.5 h) to heat the creep specimens from room temperature to 973 K (test temperature). Short-time aging (aging for 3.6 ks (1 h) at 973 K) on the solution-treated creep specimens with fine, medium. or coarse grain was made in the electric furnace of the creep–rupture equipment before loading. Some of the specimens were air-cooled after the short-time aging for microscopic observation and hardness test. The hardness of the heat-treated specimens was measured using a Vickers hardness tester (the applied load was 4.9 N). The fine-grained specimen ($d = 45.2$ μm) has the highest hardness among the heat-treated specimens (Table 1).

Figure 1 shows the optical micrographs of the specimens of the Ni–Cr alloy aged for 3.6 ks at 973 K after solution treatment. In the fine-grained specimen (Fig. 1a),

Table 1 Heat treatment, grain diameter, and hardness of the heat-treated specimens of the Ni–Cr alloy

Specimens	Heat treatment		Grain diameter, d (μm)	Hardness[a], HV (kgf/mm^2)
	Solution treatment	Aging		
Fine grain	1,423 K, 1.8 ks (0.5 h) → W.Q.	973 K, 3.6 ks (1 h) → A.C.	45.2	409
Medium grain	1,423 K, 7.2 ks (2 h) → W.Q.	973 K, 3.6 ks (1 h) → A.C.	108	360
Coarse grain	1,473 K, 14.4 ks (4 h) → W.Q.	973 K, 3.6 ks (1 h) → A.C.	286	358
Recommended aging	1,423 K, 7.2 ks (2 h) → W.Q.	1,123 K, 86.4 ks (24 h) → A.C. +973 K, 72 ks (20 h) → A.C.	108	359

W.Q. water-quenched, *A.C.* air-cooled

[a] Vickers hardness number (load 4.9 N)

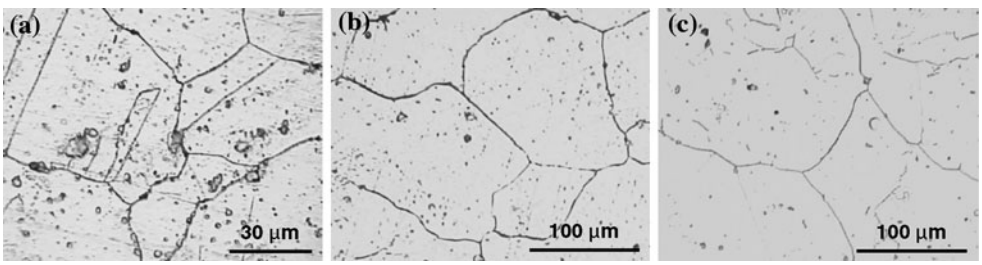

Fig. 1 Optical micrographs of the specimens of the Ni–Cr alloy aged for 3.6 ks at 973 K after solution treatment: **a** fine-grained specimen ($d = 45.2$ μm), **b** medium-grained specimen ($d = 108$ μm), **c** coarse-grained specimen ($d = 286$ μm), and (d: grain diameter)

a large amount of residual precipitates can be seen either along the grain boundaries and within the grains. Grain boundaries are slightly serrated with large residual precipitates in the fine-grained specimen. The amount of the residual precipitates is smaller in the medium-grained specimen (Fig. 1b) and in the coarse-grained specimen (Fig. 1c). Precipitates of γ' phase and $M_{23}C_6$ carbide were also found in these specimens. Chemical analysis of precipitates observed in heat-treated specimens was made using a TEM-EDS or a SEM-EDS. Dislocations and γ' phase in the grains were also examined using a TEM on some heat-treated specimens. Fracture mechanism was examined using an optical microscope and a SEM on the ruptured specimens. The hardness was also measured at the grip part of the ruptured specimens to evaluate the precipitation hardening during creep at 973 K.

Experimental results

Creep–rupture properties

Figure 2 shows the rupture-life mechanical properties of the Ni–Cr alloy at 973 K. The fine-grained specimen ($d = 45.2$ μm) has almost the same rupture life as the medium-grained specimen ($d = 108$ μm). The coarse-grained specimen ($d = 286$ μm) shows significantly short rupture life under all stresses tested and small stress dependence of the rupture life compared to other specimens. The specimen with recommended aging exhibits a slightly shorter rupture life compared to the fine-grained and medium-grained specimens with short-time aging. Further γ' phase precipitation occurred in the fine-grained specimen ($d = 45.2$ μm) and in the medium-grained specimen ($d = 108$ μm) during creep at 973 K. In fact, hardness increased from 409 HV (the heat-treated specimen) to 435 HV (the specimen ruptured at 91.4 h under a stress of 392 MPa) in the fine-grained specimens, and increased from 360 HV (the heat-treated specimen) to 396 HV (the specimen ruptured at 355.4 h under a stress of 343 MPa) in the medium-grained specimens. On the other hand, the hardness was equal to or smaller than 357 HV in the specimen with coarse grain ($d = 286$ μm) ruptured at 14.8 h under a stress of 294 MPa, and this value was almost the same as the hardness of the heat-treated specimen (358 HV). The elongation in the fine-grained specimen is larger than that in the medium-grained specimen, and comparable with that in the specimen with recommended aging. The coarse-grained specimen also shows a little larger ductility than the medium-grained specimen. This may be related to the insufficient precipitation hardening during creep and to the creep fracture mechanism in the coarse-grained specimen. The specimen with recommended aging (the hardness of the heat-treated specimen was 359 HV) may be in an over-aged state before creep–rupture experiments.

Figure 3 shows the creep curves in the specimens of the Ni–Cr alloy at 973 K. Long secondary creep regime follows after short primary creep regime in the fine-grained specimen ($d = 45.2$ μm) and medium-grained specimen

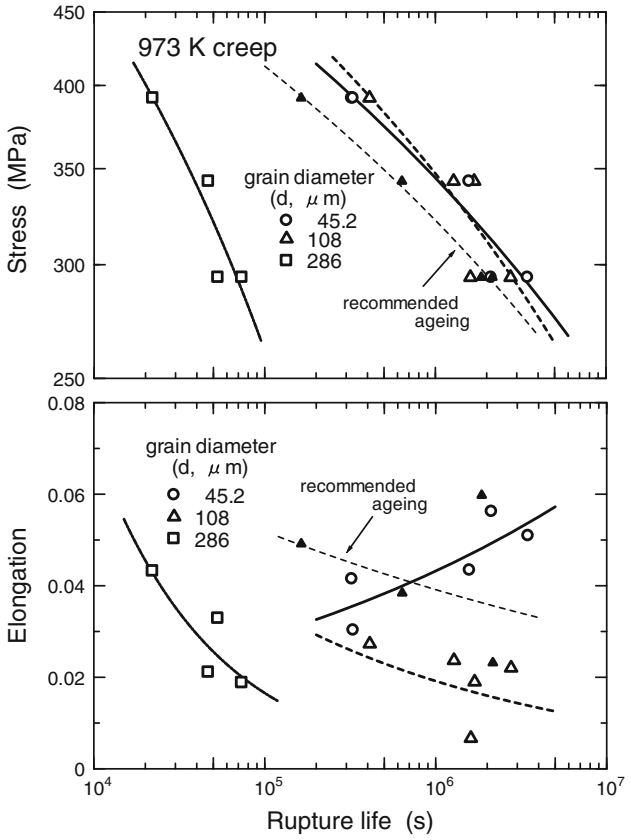

Fig. 2 Rupture-life mechanical properties of the Ni–Cr alloy at 973 K

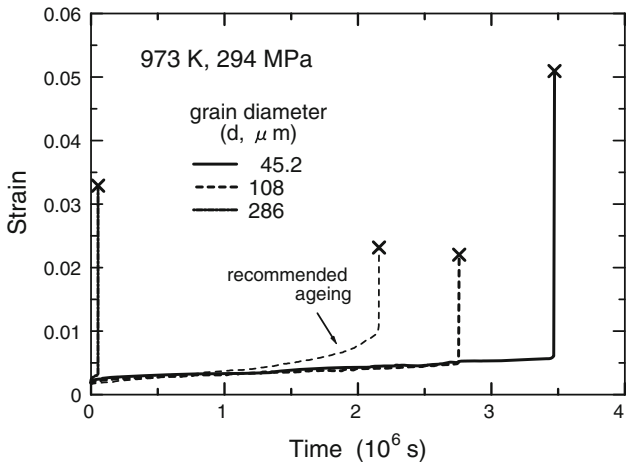

Fig. 3 Creep curves in the specimens of the Ni–Cr alloy at 973 K

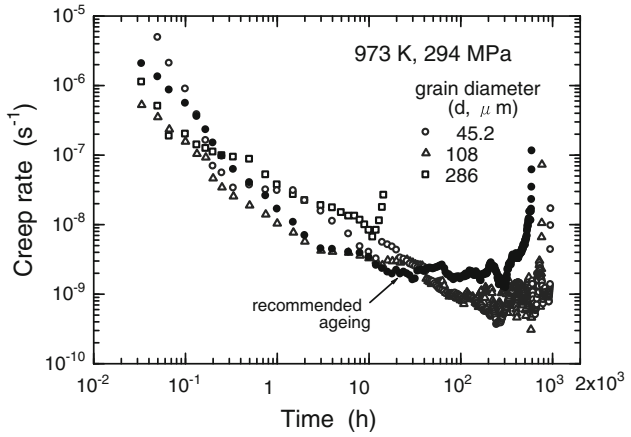

Fig. 4 Change in the creep rate with time in the specimens of the Ni–Cr alloy crept under a stress of 294 MPa at 973 K

($d = 108$ μm), while premature failure occurs in the coarse-grained specimen ($d = 286$ μm). Final fracture seems to occur after a relatively short tertiary creep regime (accelerated creep regime), whereas the specimen with recommended aging exhibits a well-defined accelerated creep regime. Figure 4 shows the change in the creep rate with time in the specimens of the Ni–Cr alloy crept under a stress of 294 MPa at 973 K. The creep rate decreases at first with increasing time (the primary creep regime) and reaches almost constant value (the minimum creep rate), and then increases abruptly to final fracture in these specimens. The minimum creep rate is higher in the coarse-grained specimen ($d = 286$ μm) in which premature failure occurred. The creep rate of the fine-grained specimen ($d = 45.2$ μm) is a slightly larger than that of the medium-grained specimen ($d = 108$ μm). Furthermore, the specimen with recommended aging shows a slightly higher minimum creep rate compared to these conditions. As described above, the hardness of the grip part of the ruptured specimens was a slightly higher than that of the heat-treated specimens in the fine-grained specimen. Relatively high creep resistance of the fine-grained specimen ($d = 45.2$ μm) may be attributed to further γ' phase precipitation caused during creep at 973 K.

Fracture mechanism

It is well known that creep ductility decreases with increasing grain size in metallic materials [11–13]. The elongation in the fine-grained specimen ($d = 45.2$ μm) was larger than that in the medium-grained specimen ($d = 108$ μm) (Fig. 2). However, the creep ductility of the coarse-grained specimen ($d = 286$ μm) was not small compared to that of the medium-grained specimen. This implies that the fracture mechanism changes as the grain size increases [10], although the principal fracture mechanism is generally intergranular fracture in polycrystalline metals and alloys at high temperatures. Figure 5 shows the optical and scanning electron micrographs after failure under a stress of 294 MPa at 973 K. Tensile direction is horizontal in the optical micrographs (Fig. 5a, c, e). Grain-boundary cracks linked to the fracture surface are observed both in the fine-grained specimen (Fig. 5a) and in the medium-grained specimen (Fig. 5c), and a transgranular crack is visible in the vicinity of a grain boundary in the coarse-grained specimen (Fig. 5e). A secondary crack can be seen on grain boundaries in the fine-grained specimen (Fig. 5a), while no secondary cracks are detected in the medium-grained specimen and coarse-grained specimen. The fine-grained specimen shows a ductile intergranular fracture surface with dimples which are associated to large residual precipitates on grain boundaries (indicated by arrows in Fig. 5b), while the medium-grained specimen exhibits a brittle intergranular fracture surface (Fig. 5d). The fracture surface of the coarse-grained specimen consists of transgranular fracture region with small dimples (indicated by TG in Fig. 5f) and brittle intergranular fracture region (indicated by IG in Fig. 5f). Therefore, a relatively large creep ductility in the coarse-grained specimen is attributed to the occurrence of transgranular fracture. However, the double aging did not increase the rupture life of the specimens in comparison with short-time aging for 3.6 ks at 973 K (Fig. 2) in the Ni–Cr heat-resistant alloy because of over-aging of the specimen. Brittle intergranular fracture also occurred in the specimen with recommended aging, although this specimen exhibited a relatively large elongation owing to over-aging (Fig. 2).

Discussion

The hardness of fine-grained specimen ($d = 45.2$ μm) is higher than that of other specimens after short-time aging (aging for 3.6 ks at 973 K) (Table 1). This may be related to precipitation of γ' phase [7, 8] or formation of dislocation substructure [14–16], although residual precipitates, $M_{23}C_6$ carbide and grain refinement may also have some effects on the hardening of specimens. Figure 6 shows the transmission electron micrographs of the specimens of the wrought Ni–Cr alloy aged for 3.6 ks at 973 K. According to the results of the TEM-EDS analysis on the heat-treated specimens, grain-boundary precipitates are considered to be $M_{23}C_6$ carbide [7, 8] (Fig. 6a, b). Dislocation density is very low and characteristic dislocation substructure is not observed in the interior of grains in both the fine-grained specimen ($d = 45.2$ μm) (Fig. 6a) and the medium-grained specimen ($d = 108$ μm) (Fig. 6b). Thus, the high hardness of the fine-grained specimen cannot be obtained from

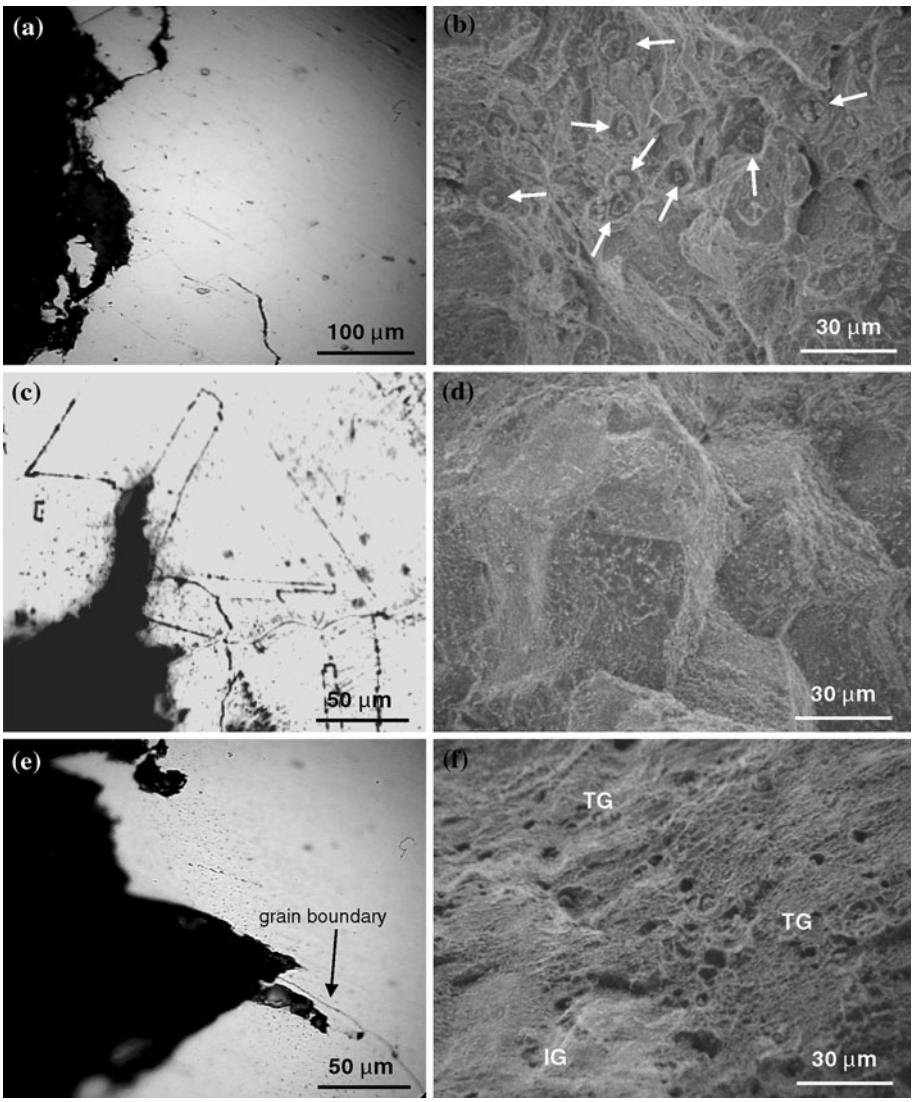

Fig. 5 Optical and scanning electron micrographs after failure under a stress of 294 MPa at 973 K. **a**, **b** shows fine-grained specimen ($d = 45.2$ μm); **c**, **d** medium-grained specimen ($d = 108$ μm); and **e**, **f** coarse-grained specimen ($d = 286$ μm) (d: grain diameter) (*arrows* indicate residual precipitates, *TG* shows the transgranular fracture region, and *IG* indicates the brittle intergranular fracture region)

dislocation substructure. Very fine precipitates are visible in the grains of the heat-treated specimens at the higher magnifications (Fig. 6c), and are identified as γ' phase from the selected area electron diffraction pattern (Fig. 6d).

It is considered from the results of the SEM-EDS and TEM-EDS analyses that the residual precipitates are primarily MC-type carbide containing large amounts of Nb and Ti in the wrought Ni–Cr alloy [7, 8]. It is known that γ' particles are also formed by heat treatments at high temperatures above about 1,033 K from MC-type residual precipitates by the following chemical reaction (γ is the fcc matrix) [7, 8].

$$MC + \gamma \rightarrow M_{23}C_6 + \gamma' \quad (1)$$

The above chemical reaction may promote the precipitation of γ' particles in specimens which involve the larger amount of residual precipitates during aging for 3.6 ks at 973 K. The highest hardness (409 HV) in the fine-grained specimen in the as-heat-treated condition (Table 1) is attributed for the most part to the larger amount of γ' precipitates (Fig. 6). The above chemical reaction is more likely to occur in the specimens with the smaller grain sizes during short-time aging, because grain-boundary diffusion facilitates the migration of atoms. The hardness increased in the fine-grained specimen ($d = 45.2$ μm) and in the medium-grained specimen ($d = 108$ μm) during creep. The separate nucleation and growth of γ' phase particles as well as the above chemical reaction may occur in the specimens during creep at 973 K. Specimens with the smaller grain sizes generally exhibit the better creep ductility [11–13]. Thus, the fine-grained specimen has a combination of high creep resistance and good creep ductility (Figs. 2 and 4). The amount of MC-type residual carbide is smaller, and the effect of grain-boundary diffusion on the migration of atoms is smaller in the specimens with the larger grain sizes. Therefore, the chemical reaction (Eq. 1) is less likely to occur in the coarse-grained specimen during short-time aging or during creep at 973 K. This

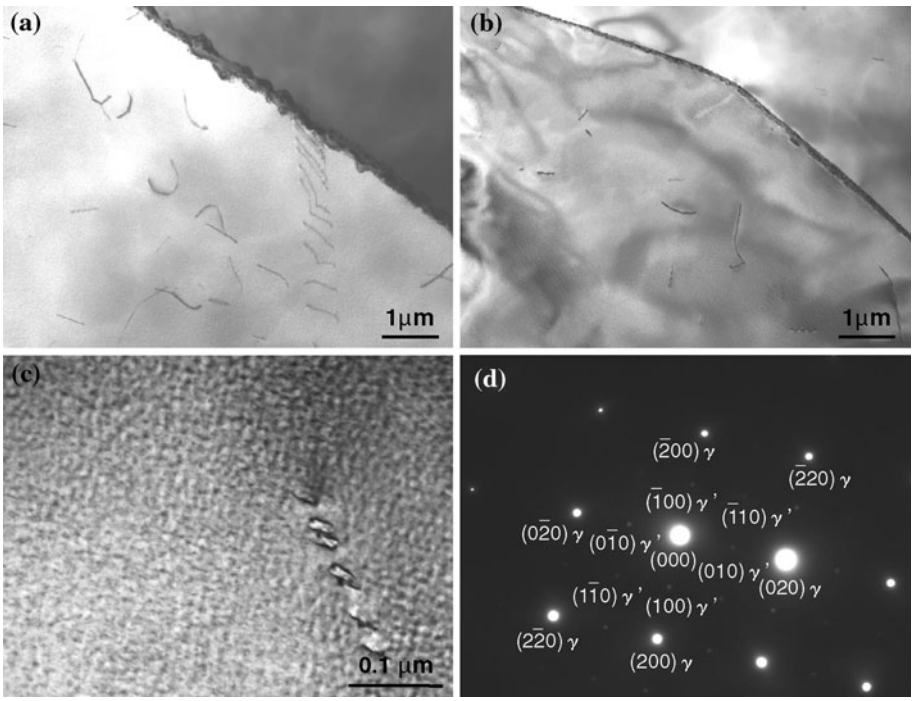

Fig. 6 Transmission electron micrographs of the specimens of the wrought Ni–Cr alloy aged for 3.6 ks at 973 K. **a**, **c**, **d** fine-grained specimen ($d = 45.2$ μm), **b** medium-grained specimen ($d = 108$ μm) ((**a**)–(**c**) are bright field images, and (**d**) is the selected area electron diffraction pattern of (**c**)) (d: grain diameter)

may lead to insufficient precipitation hardening in the coarse-grained specimen and may result in a premature creep failure (Fig. 2).

Many large residual precipitates were observed on the fracture surface of the fine-grained specimen (Fig. 5b), although some of them may have disappeared by the above chemical reaction during aging and creep at 973 K. Using a micromechanics model, K. Tanaka et al. [17] showed that the crack can initiate by stress concentration at non-deforming particles embedded in a ductile matrix owing to plastic deformation under a uniaxial tensile stress. They found that the fracture strain (plastic strain to crack initiation) is inversely proportional to the square root of the particle size. Therefore, large residual precipitates are also expected to become potential nucleation sites for grain-boundary cracks at high temperatures where the effect of grain-boundary sliding on the creep deformation becomes prominent [18]. Nevertheless, the residual precipitates did not deteriorate the creep–rupture properties in the fine-grained specimen at 973 K (Fig. 2). According to another micromechanics model in which the effect of recovery by atomic diffusion is taken into account [19, 20], the stress concentration at the residual precipitates can be reduced by diffusion of atoms and the creep strain to crack initiation can increase as deformation temperature increases. Decrease of the stress concentration may be more prominent in specimens with the smaller grain sizes, in which the recovery process can be enhanced by grain-boundary diffusion of atoms. These conditions can qualitatively explain why the residual precipitates did not impair the rupture properties in the fine-grained specimen.

According to Garofalo et al. [9], if grain boundaries act as sources and sinks of dislocations, then the steady-state creep rate is proportional to $1/d$ (d: grain diameter). This explains why the minimum creep rate of the fine-grained specimen is larger than that of the medium-grained specimen (Fig. 4). The rupture life of the fine-grained specimen is almost equal to that of the medium-grained specimen (Fig. 2). The product of minimum creep rate ($\dot{\varepsilon}_s$) and rupture life (t_r), $\dot{\varepsilon}_s \cdot t_r$, gives a measure of creep ductility, and this value is larger in the fine-grained specimen than in the medium-grained specimen. Further, ductile intergranular fracture with dimples occurred in the fine-grained specimen, while brittle intergranular fracture was observed in the medium-grained specimen (Fig. 5). These are responsible for the better ductility of the fine-grained specimen.

It is known that serrated grain boundaries are formed by heat treatments [2, 21–24] and can improve creep properties in heat-resistant alloys [2, 22, 23]. The strengthening effect of serrated grain boundaries results from the inhibition of grain-boundary sliding which governs the initiation and growth of cracks and the retardation of brittle intergranular fracture [22, 23]. It is also known that discrete MC carbides and dendritic γ' phase which form serrated grain boundaries are responsible for the improved creep resistance of a nickel-based alloy containing Hf [25]. In the fine-grained specimen, grain boundaries are slightly

serrated with large residual precipitates (Fig. 1a) and ductile intergranular fracture with dimples occurred in creep at 973 K (Fig. 5b). Therefore, the strengthening mechanism similar to serrated grain boundaries may operate in the fine-grained specimen. Fine grain size is also favorable for improved creep strength [1]. The fine-grained specimen that is produced by combination of short-time solution treatment and short-time aging, exhibited better creep properties than the specimen with recommended double aging. Such a simple heat treatment is applicable to high-temperature components of wrought Ni–Cr alloys.

Conclusions

The effect of heat treatments on the creep–rupture properties was investigated using a wrought Ni–Cr (Inconel X-750 type) heat-resistant alloy at 973 K. Short-time aging for 3.6 ks at 973 K was made on the solution-treated specimens with different grain sizes. The results obtained are summarized as follows:

(1) The fine-grained specimen ($d = 45.2$ μm) with short-time solution treatment exhibited a combination of high creep resistance and good creep ductility. The fine-grained specimen had almost the same rupture life and superior creep ductility as those of the medium-grained specimen ($d = 108$ μm) with normal solution treatment. The fine-grained specimen and medium-grained specimen showed the longer rupture life compared with the specimen with recommended aging. The coarse-grained specimen ($d = 286$ μm) with high-temperature long-time solution treatment had very short rupture life because of insufficient precipitation hardening after short-time aging and during creep at 973 K.

(2) Ductile intergranular fracture with dimples occurred in the fine-grained specimen, while brittle intergranular fracture was observed in the medium-grained specimen, and in the specimen with recommended aging. Both transgranular fracture and brittle intergranular fracture were observed in the coarse-grained specimen with short-time aging.

(3) The principal strengthening of specimens was attributed to the precipitation hardening by γ' phase particles. The fine-grained specimen had the highest hardness in all the specimens, and the increase of the hardness was observed both in the fine-grained specimen and in the medium-grained specimen during creep. A simple heat treatment composed of short-time solution treatment (heating for 1.8 ks (0.5 h) at 1,423 K) and short-time aging (aging for 3.6 ks at 973 K), is applicable to high-temperature components of wrought Ni–Cr alloys.

Acknowledgements The authors thank Dr. D. Fujishiro, Former Director of Nittan Valve Company, for supplying Ni–Cr alloy used in this study. They also thank Prof. Z. Nakagawa and Mr. K. Sasaki of Center for Geo-Environmental Science, Akita University for chemical analysis by SEM-EDS, and Mr. T. Moronaga of Electronics Division of Kobelco Research Institute Inc. for microstructural and chemical analyses using TEM-EDS.

References

1. Donachie M, Donachie S (2002) Superalloys, 2nd edn. ASM International, Materials Park, Ohio
2. Wisniewski A, Beddoes J (2009) Mater Sci Eng A 510–511:266
3. Raymond EL (1967) Trans Metall Soc AIME 239(9):1415
4. Venkiteswaran PK, Taplin DMR (1974) Met Sci 8(1):97
5. Arbel A, Pande CS (1988) J Mater Sci 23(9):3375. doi:10.1007/BF00551321
6. Jahazi M, Mashreghi AR (2002) Mater Sci Technol 18(4):458
7. Sims CT, Hagel WC (1972) The superalloys. Wiley, New York
8. Sims CT, Stoloff NS, Hagel WC (1987) Superalloys II. Wiley, New York
9. Garofalo F, Domis W, von Gemmingen F (1964) Trans Met Soc AIME 230(10):1460
10. Tanaka M, Kato R, Ito Y, Kayama A (2000) Z Metallkd 91(5):429
11. Lagneborg RJ (1969) J Iron Steel Inst 207(11):1503
12. Barrett CR, Lytton JL, Sherby OD (1967) Trans Met Soc AIME 239(1):170
13. Evans HE (1984) Mechanisms of creep fracture. Elsevier Applied Science Publishers, London
14. McElroy RJ, Szkopiak ZC (1972) Int Metall Rev 17:175
15. McQueen HJ (1977) Metall Trans A 8A(6):807
16. Hausselt JH, Nix WD (1977) Acta Metall 25(6):595
17. Tanaka K, Mori T, Nakamura T (1970) Philos Mag 21(170):267
18. Langdon TG, Vastava RB (1982) ASTM STP 765. ASTM, Philadelphia, p 435
19. Tanaka M, Iizuka H (1985) J Mater Sci 20(10):3750. doi:10.1007/BF01113784
20. Iizuka H, Tanaka M (1986) J Mater Sci 21(2):611. doi:10.1007/BF01145531
21. Koul AK, Gessinger GH (1983) Acta Metall 31(7):1061
22. Iizuka H, Tanaka M (1986) J Mater Sci 21(8):2803. doi:10.1007/BF00551493
23. Tanaka M, Miyagawa O, Sakaki T, Iizuka H, Ashihara F, Fujishiro D (1988) J Mater Sci 23(2):621. doi:10.1007/BF01174696
24. Hong HU, Nam SW (2002) Mater Sci Eng A 332:255
25. Kotval PS, Venables JD, Calder RW (1972) Metall Trans 3(2):453